Mechanical properties of ultrananocrystalline diamond prepared in a nitrogen-rich plasma: A theoretical study

Jeffrey T. Paci,[1,*] Ted Belytschko,[2] and George C. Schatz[1,†]
[1]*Department of Chemistry, Northwestern University, 2145 Sheridan Road, Evanston, Illinois 60208-3113, USA*
[2]*Department of Mechanical Engineering, Northwestern University, 2145 Sheridan Road, Evanston, Illinois 60208-3111, USA*
(Received 27 April 2006; revised manuscript received 5 September 2006; published 13 November 2006)

We examine the mechanical properties of ultrananocrystalline diamond (UNCD) produced by plasma-enhanced chemical vapor deposition, with a focus on thin films created with high levels of nitrogen in the plasma. A model with several of the attributes of the corresponding experimental UNCD is developed and its properties explored. Simulations are performed using semiempirical quantum mechanics and density functional theory. Our results predict a Young's modulus of 0.69 TPa, failure strain of 0.13, and a tensile fracture stress of 61 GPa which are 66%, 100%, and 61%, respectively, of those predicted for UNCD produced in the absence of nitrogen. As in the case of UNCD produced without nitrogen in the plasma deposition, the fracture stress (σ_f=61 GPa) is very large compared to that observed experimentally; these indicate that the experimental specimens contain large defects and some estimates are made of the size of these defects using the Griffith formula with the surface energy computed here. The effect of nitrogen on the mechanical properties of atom-wide UNCD grain boundaries is also investigated. Throughout, the accuracy of the various simulation methods is compared and evaluated.

DOI: 10.1103/PhysRevB.74.184112 PACS number(s): 62.20.Mk, 62.25.+g, 81.05.Uw

I. INTRODUCTION

Plasma-enhanced chemical vapor deposition techniques can be used to make thin diamond films composed of extremely small (3–5 nm) diamond grains and atom-wide grain boundaries (~0.2–0.4 nm wide).[1–4] The material, which is called ultrananocrystalline diamond (UNCD), has very impressive mechanical properties (hardness, fracture stress, smoothness).[5–8] Adding nitrogen to the plasma used to make these films has a dramatic effect on their electrical conductivity.[9–14] Because of these properties, UNCD is an excellent candidate for use in the production of microelectromechanical and nanoelectromechanical systems.[15,16]

Low-level plasma-nitrogen films have morphologies which are similar to those produced in the absence of nitrogen. However, the structure of UNCD changes significantly as the level of nitrogen in the plasma is increased above 5%.[10] Grain boundaries (GB's) become significantly wider, and the average single-crystal diamond (SCD) grain size increases. For example, films produced using 20% plasma nitrogen have GB's which are ~2 nm wide and average grain sizes of 16 nm.[13]

Increased plasma-nitrogen levels also result in an increased GB volume fraction. This fraction can be estimated using[17]

$$V^{\mathrm{GB}} = \frac{3\Delta(d-\Delta)^2}{d^3}, \tag{1}$$

where Δ is the GB thickness and d the average grain diameter. For UNCD produced without nitrogen in the plasma, $\Delta \sim 0.3$ nm and $d \sim 4$ nm, which suggests a $V^{\mathrm{GB}}=0.19$, and 20% plasma-nitrogen films have a $\Delta \sim 2$ nm and $d \sim 16$ nm, so $V^{\mathrm{GB}}=0.29$.

The differences in volume fraction and average grain size suggest that whereas for films produced in the absence of plasma nitrogen one can envision a material in which grains essentially butt up against each other, high-level plasma-nitrogen films are better envisioned as diamond grains embedded in large amounts of GB material.

The GB's are composed of a mix of sp^2- and sp^3-hybridized carbon.[13] Near-edge x-ray-absorption fine-structure spectroscopy suggests that 13.5% of the carbon in films produced with 20% plasma nitrogen is sp^2 hybridized.[13] Assuming that all of the sp^2 carbon is confined to the GB's, this 13.5% value suggests that 0.135/0.287 or 47% of GB carbon atoms are sp^2 hybridized.

Some nitrogen is incorporated into UNCD films produced with nitrogen in the plasma. High-resolution secondary-ion-mass spectroscopy indicates that the level of nitrogen in the films is a maximum when they are grown with 18% plasma nitrogen.[13] At this nitrogen level, the nitrogen concentration in the resulting films is 2.2×10^{20} cm^{-3} (1–2 nitrogen atoms per 1000 carbon atoms). The nitrogen is thought to be present at the GB's rather than being within the SCD grains.[18]

The presence of SCD grains cemented to each other by wide GB layers (which have widths which are on the same length scale as the grain radii) makes nitrogen-rich plasma UNCD films a kind of composite material. These films are different than most composites in that the distinct materials are, in this case, both made of carbon atoms, whereas in most others, each component has a higher level of chemical distinctness. Nevertheless, this UNCD is composed of grains which are SCD like and of GB's which exhibit, because of their high level of sp^2 hybridization, some properties which are not exhibited by other diamond thin films.

There appears to be excellent connectivity between the two phases, resulting in a material that is extremely stiff and strong. For example, UNCD has a Young's modulus[19] E =0.850 TPa and a tensile fracture stress[19] σ_f=2–3 GPa. Both of these values approach those of natural diamond[20–22] ($E \sim 1$ TPa and $\sigma_f \sim 4$ GPa).

Although UNCD produced without nitrogen in the plasma is an electrical insulator, films produced using plasma nitrogen are good conductors. The former have a conductivity[10] $\sigma_e \sim 1 \times 10^{-3}\ \Omega^{-1}\ \mathrm{cm}^{-1}$. Increasing levels of plasma nitrogen cause an increase in conductivity of the resulting film, with 20% plasma-nitrogen films having a $\sigma_e = 143\ \Omega^{-1}\ \mathrm{cm}^{-1}$.[10] Pure polycrystalline graphite (PCG) (which contains approximately 100% sp^2 carbon) has a $\sigma_e = 300\ \Omega^{-1}\ \mathrm{cm}^{-1}$; high levels of plasma nitrogen result in films with conductivities approximately half that of PCG.

There is significant evidence to suggest that it is the sp^2-carbon network in UNCD, and not the presence of nitrogen, that is most responsible for the conductivity of these films. A hydrogen treatment can be used to convert carbon hybridization from sp^2 to sp^3. When plasma-nitrogen UNCD is subjected to such a treatment, the films become electrically insulating.[23] The fact that there are only 1–2 nitrogen atoms per 1000 carbon atoms in the films, that what nitrogen is in the films seems to be located at the GB's, and that nitrogen when introduced into a SCD lattice tends to form a deep donor (1.4 eV below the conduction band) (Ref. 24) all suggest that the presence of nitrogen in the films is not a major contributor to their electrical conductivity.

In order to elucidate the mechanical properties of plasma-nitrogen UNCD, it is necessary to develop an understanding of the role defects play in the failure of the material. The tensile fracture stress of natural diamond is much smaller than the theoretical value for SCD. The theoretical $\sigma_f = 225$, 130, and 90 GPa for SCD strained in the [100], [110], and [111] directions, respectively.[25] Using the results of a large number of diamond indentation studies, Field and Pickles[22] estimate the tensile fracture stress of natural diamond (to the best of our knowledge, the results of tensile fracture stress measurements on natural diamond have never been reported). They predict a $\sigma_f \sim 4$ GPa by assuming a defect size of 1 μm; this is the typical size of defects found in specimens of natural diamond.[22] These defects, often sharp ended, lead to stress concentrations near their tips and to the subsequent failure of the material. UNCD also contains defects of significant size,[6] which play an important role in fracture.[26] The impact of these defects on σ_f in a brittle solid like diamond can often be well described by Griffith theory.[27]

There are a variety of theoretical methods available for studying the mechanical properties of diamond and UNCD films. Self-consistent density functional theory (DFT) methods are widely used in investigations of this kind. They are computationally demanding but provide accurate estimates of those mechanical properties which depend on atomic structures near equilibrium geometries (e.g., E). The accuracy with which they are able to predict properties which depend on geometries and energies when bonds are extended close to their breaking point (e.g., σ_f and failure strain ϵ_f) is not as certain.[28] However, most bonds are extended by up to about $\sim$15% before fracture; i.e., they are not that elongated. This means that whatever problems DFT has near fracture are not very important. Overall, self-consistent DFT methods are usually the most accurate and computationally practical methods available for mechanical property investigations.

Semiempirical quantum mechanical schemes such as intermediate neglect of differential overlap (INDO) and self-consistent-charge density-functional tight-binding (SCC-DFTB) schemes, have been parametrized to reproduce DFT calculations and often produce high-quality results. They do, however, suffer from certain shortcomings. Their small basis sets, and the modeling or neglect of certain interactions in an effort to speed computational execution, can result in geometries and/or interatomic interactions which are less accurate than self-consistent DFT.

The purpose of this paper is to provide insight into the mechanical properties of UNCD films produced with high levels of nitrogen and to compare various computational methods in order to evaluate their accuracy. The effect of nitrogen substitution at atom-wide GB's is also investigated. To do this, we present models of these UNCD films which we strain-to-failure, calculating structures and energies using semiempirical quantum mechanics and DFT.

We investigate two models of nitrogen doping, the second being the more interesting of the two. In the first, nitrogen is placed at atom-wide GB's. The purpose of this model, which is not specific to UNCD, is to provide insight into the effect of nitrogen on the mechanical properties of diamond GB's. In the second model, an amorphous carbon region is placed at the GB and no nitrogen atoms are included. This second GB model has several of the attributes of GB's found in high-level plasma-nitrogen UNCD and, therefore, can be used as a better indicator than the first model of the mechanical properties of the intergranular material in these UNCD films.

The remainder of the paper is organized as follows. In Sec. II, the semiempirical quantum mechanical and DFT methods are described. The models used for, and results derived from straining UNCD with various amounts of nitrogen at atom-wide GB's, are the subject of Sec. III. In Sec. IV, the more realistic high-level plasma-nitrogen UNCD GB model is described. The results of straining this model to failure are examined. In addition, a Griffith formula is used to estimate the impact of crack propagation on σ_f in plasma-nitrogen films. A summary is provided in Sec. V.

II. SIMULATION METHODS

Density functional theory calculations were performed using the Spanish initiative for electronic simulations with thousands of atoms (SIESTA).[29,30] This self-consistent DFT program uses numerical orbital basis set functions and norm-conserving pseudopotentials. Basis sets including multiple-ζ and polarization orbitals are available. Both local density and generalized gradient (GGA) approximations to the exchange-correlation energy are provided. The code contains both diagonalization and order-N-scaling algorithm options for solving the Kohn-Sham equations.

We have used the Perdew-Burke-Ernzerhof (PBE) GGA functional and a double-ζ plus polarization basis set for our SIESTA calculations. Pulay mixing at levels as high as 10 was used, and reductions of the default electron density matrix mixing weight (to weights as low as 0.1) were made, whenever necessary to facilitate convergence of the self-consistent field (SCF) cycles. Conjugate gradient geometry optimizations of atomic positions were performed in all simulations

except those for which we indicate otherwise. The Γ point was used for Brillouin zone sampling and diagonalization to solve the Kohn-Sham equations.

We performed a small number of calculations in which an additional *k*-space point was used for sampling. The resulting structures and energies were not significantly different than those of corresponding calculations in which only the Γ point was used.

A density-functional-based tight-binding program with self-consistent charges[31,32] (SCC-DFTB) has also been used for some of our simulations. The method on which the program is based is a two-centered approach to DFT. In it, the Kohn-Sham density functional is expanded to second order around a reference electron density. This density is obtained from self-consistent DFT calculations for weakly confined neutral atoms using the GGA. The confinement potential is optimized and a minimal valence basis set used to calculate one- and two-centered tight-binding matrix elements within DFT.

MSINDO (Ref. 33) is a semiempirical SCF molecular orbital package in which the INDO approximation is implemented. The program can be used to calculate properties of molecular systems containing first through third row elements. Bulk systems can be simulated using an embedding procedure or the cyclic cluster model (CCM). We use the CCM, the essence of which is the creation of identical environments for translationally equivalent cluster atoms.

We have shown in Ref. 26 that calculating the geometry of structures with MSINDO and their energies using the PBE method provides quite accurate predictions of the mechanical properties of UNCD (produced without nitrogen in the plasma) and SCD. The method, which we named PBE//MSINDO, is much more accurate than MSINDO alone and only marginally more computationally expensive. In addition, it requires an order of magnitude less computer time than when geometry optimizations and energy evaluations are both performed using PBE simulations.[26] For these reasons, we report results obtained by using this hybrid method instead of those calculated using only MSINDO.

The SCC-DFTB method was selected because it has been used previously to provide valuable insight into the properties of diamond structures containing GB's with and without nitrogen doping.[18] In addition, it has been shown to give results in good agreement with higher-level quantum-chemical methods for other systems composed of carbon and nitrogen.[34]

In all of our calculations, the clusters are strained using algorithms which incrementally move planes of atoms apart. After each strain increment (which is accompanied by a corresponding increase in the size of the unit cell) the positions of all atoms are geometry optimized. The applied force is calculated from the change in energy of the cluster caused by adding an increment of strain, using finite difference. Young's-modulus values are calculated by parabolic fits to energy versus strain data. A failure strain is defined as the strain immediately following the maximum in the slope of an energy versus strain curve. A tensile fracture stress is calculated using the force corresponding to this maximum slope. Full details of these methods can be found in Ref. 26.

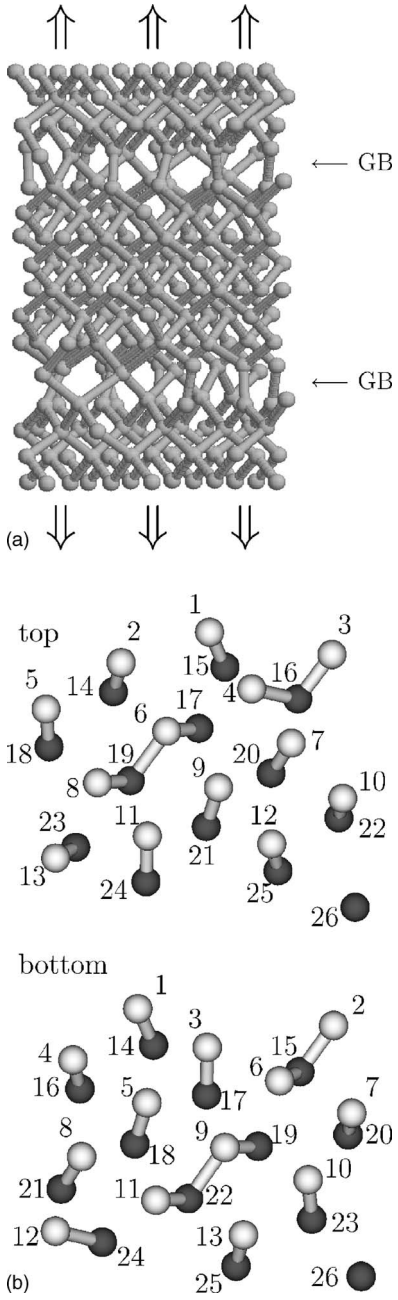

FIG. 1. (a) The cluster model for nitrogen-doped UNCD GB's. This cluster is initially under zero strain. The horizontal arrows indicate the locations of the two GB's (GB). The vertical arrows indicate the direction of applied strain. (b) Top view of GB's: the numbering scheme used to identify specific GB atoms. The top (bottom) panel shows the top (bottom) GB atoms. The light (dark) gray circles represent GB atoms in the plane which is the closest (farthest) of each pair of planes to (from) the top of the cluster. The GB's have been rotated slightly to make the location of individual atoms more clearly visible.

III. EFFECT OF NITROGEN AT GRAIN BOUNDARIES

Although only small amounts of nitrogen are incorporated in UNCD even when high levels of plasma nitrogen are used in its preparation, there is interest in the effect of nitrogen on the strength of UNCD GB's and diamond films in general. In

this section we study only the effect of added nitrogen at the GB, while assuming that the GB structure is the same as in undoped UNCD.

We have chosen the Σ 13 twist (100) GB structure for this study, as high-energy twist GB's, of which this is an example, are the most common type of GB found in UNCD.[35] The cluster used in our simulations is shown in Fig. 1(a). To produce models corresponding to different levels of doping, nitrogen atoms have been substituted for carbon atoms at various GB locations. These locations have been chosen at random, with the specific locations chosen shown in Table I. This table is to be used in conjunction with Fig. 1(b) which shows the GB-atom numbering scheme.

Doping levels of 4, 8, 16, and 32 nitrogen atoms per 208-atom cluster have been considered. As Fig. 2(a) indicates, increased levels of nitrogen mean that less energy is required to break the structures. Considering only the PBE//MSINDO results at this point, Table II indicates that the fracture stresses decrease with increasing nitrogen levels. Failure strains and E values tend to decrease with increased levels of nitrogen although not monotonically, with E values only weakly effected by nitrogen substitution.

We do not present stress-strain curves. Stresses are calculated by finite difference, using energy-strain data.[26] The jagged nature of this data, the result of abrupt changes in geometry as the system is strained due to changes in fracture path,[36] leads to discontinuous stress-strain data. Instead, fracture stresses are presented in tabular form (see Table II).

An examination of the structures indicates that nitrogen interrupts the sp^3-hybridized bonding in UNCD, resulting in fewer bonds across the GB's. This occurs because nitrogen tends to form no more than three covalent bonds with its near neighbors while carbon can form as many as four. In addition, carbon-carbon bonds (bond enthalpy of ~350 kJ/mol for single and ~615 kJ/mol for double bonds) are replaced by weaker carbon-nitrogen (~290 kJ/mol) and nitrogen-nitrogen (160 kJ/mol) single bonds, as nitrogen is substituted. Because of these factors, nitrogen-doped structures have smaller fracture stresses than undoped UNCD. However, the weakening of the structure, when even large amounts of nitrogen (32 nitrogen atoms per 208-atom cluster) are substituted, is modest. Young's modulus, ϵ_f and σ_f are 92%, 70%, and 68% of the respective undoped UNCD values.

The mechanical properties are somewhat effected by the locations chosen for nitrogen substitution, as illustrated in Fig. 2(b). This figure shows energy-strain behavior resulting from applying strain to five different clusters, each containing four nitrogen atoms. The specific locations chosen for substitution are presented in Table I and Fig. 1(b). The atomic positions shown in the figure differ slightly from those in the unstrained structures in the simulations because small geometry changes occur upon substitution; the structures shown in Figs. 1(a) and 1(b) correspond to the optimized undoped geometry.

The weakest structures (those with the smallest ϵ_f and σ_f values) are those with nitrogen substituted at locations 1 and 4, while the strongest is that formed with nitrogen atoms at locations 3. Although there does not seem to be a quantitative way of predicting the effect of doping at a particular set

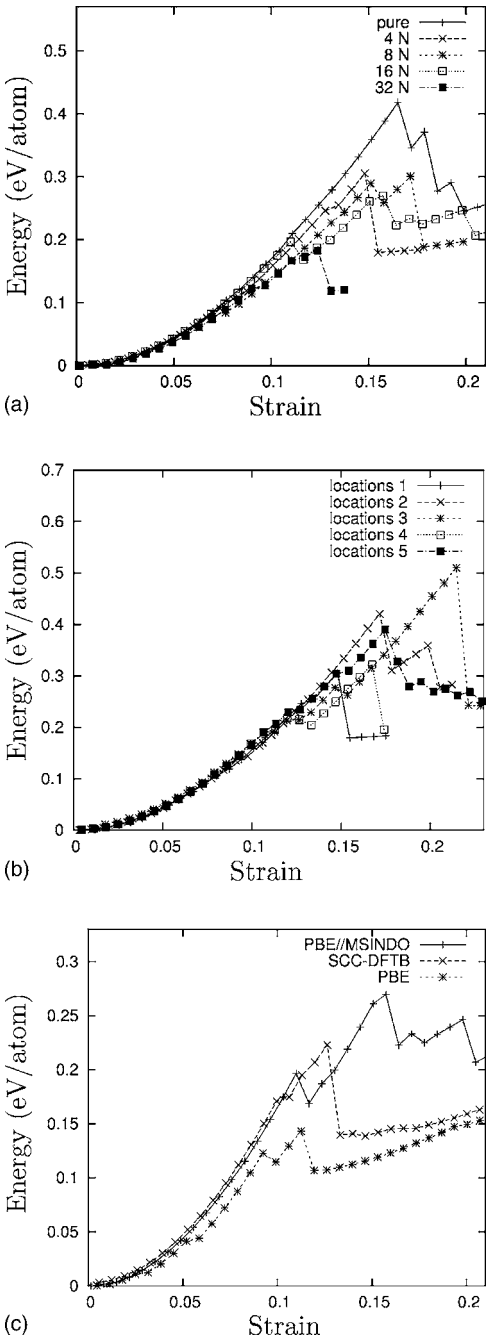

FIG. 2. Energy versus strain for (a) the different levels of nitrogen doping and (b) four nitrogen atoms placed at five different sets of GB locations. These calculations were performed with PBE//MSINDO. In (c) the PBE//MSINDO result for 16 atoms at the GB's is presented for comparison with the results of SCC-DFTB and PBE simulations performed on the same GB model.

of locations, there appears to be a relationship between the density of nitrogen atoms and strength. In general, structures in which nitrogen atoms are well separated from each other tend to be stronger than structures in which they are in closer proximity. For example, if one calculates the sum of the separations between pairs of nitrogen atoms at GB's (including consideration of the periodic boundary conditions) in a given structure, the order of structures (from smallest to larg-

TABLE I. The location of nitrogen atoms at the GB's in the nitrogen-doped cluster models. The abbreviation "t" ("b") indicates that the atom is located in the top (bottom) GB. This table is to be used in conjunction with Fig. 1(b).

Cluster	N locations	Cluster	N locations
4 N (locations 1)	t11, t19, b5, b18	8 N	t9, t11, t19, t23, b5, b9, b17, b18
4 N (locations 2)	t4, t17, b8, b14	16 N	t2, t9, t11, t12, t14, t19, t23, t25,
4 N (locations 3)	t9, t18, b9, b21		b3, b5, b9, b13, b17, b18, b21, b23
4 N (locations 4)	t1, t15, b12, b16	32 N	t2, t5, t7, t9, t10, t11, t12, t13,
4 N (locations 5)	t7, t14, b11, b26		t14, t17, t18, t19, t21, t23, t24, t25,
			b2, b3, b5, b6, b9, b10, b11, b13,
			b15, b16, b17, b18, b20, b21, b23, b25

est sum) is locations 1, 4, 2, 3, and 5. This roughly corresponds to the order of increasing σ_f (locations 4, 1, 5, 2, and then 3) and ϵ_f (locations 1, 4, 2, 5, and then 3). This correlation may be due to the fact that materials containing a small number of large defects (a pair of closely separated nitrogen atoms being a kind of relatively large defect) tend to be weaker than structures containing a large number of small defects (an isolated nitrogen atom being a kind of small defect).[27]

We move now to an evaluation of the various methods used in the simulations. The accuracy with which semiempirical methods and DFT are able to predict the mechanical properties of SCD has been evaluated elsewhere.[26] The PBE method was found to reproduce the experimental value of E [E(expt)=1.05 TPa (Refs. 20 and 21) versus E(PBE) =1.09 TPa] and the results of other DFT simulations for σ_f [σ_f=225 GPa (Ref. 25) versus σ_f=233 GPa] reasonably well. The two DFT methods predict identical ϵ_f values (ϵ_f =0.35). The semiempirical method PBE//MSINDO was found to predict these quantities with semiquantitative accuracy (E=1.01 TPa, ϵ_f=219 GPa, and ϵ_f=0.37).

Similarly, the accuracy with which PBE//MSINDO predicts the fracture properties of nitrogen-doped GB's can be determined by making comparison to simulations performed using the PBE method. Such a comparison is shown in Fig. 2(c) where results of straining the cluster doped with 16 nitrogen atoms are shown. These PBE simulations should predict accurate E values, as mentioned earlier. They indicate that PBE//MSINDO slightly underestimates this property (E=0.94 TPa versus 0.99 TPa). PBE//MSINDO predicts ϵ_f and σ_f values which are larger than the PBE values (ϵ_f =0.11 versus 0.09 and σ_f=84 versus 73 GPa). As the PBE method is expected to overbind,[28] it is reasonable to suggest that the values of ϵ_f and σ_f it predicts are high, and so PBE//MSINDO is probably somewhat less accurate at predicting these quantities than a direct comparison of PBE//MSINDO to PBE suggests.

The result of a SCC-DFTB simulation is also shown in Fig. 2(c). This predicts E, ϵ_f, and σ_f values which are closer to the PBE results than PBE//MSINDO, for the 16-nitrogen-atom cluster. However, this better accuracy is not a general feature of SCC-DFTB versus PBE//MSINDO, as the undoped UNCD cluster [the cluster shown in Fig. 1(a) with no nitrogen substitution] results for ϵ_f and σ_f, shown in Table II, indicate. The PBE method tends to overbind but SCC-DFTB predicts even larger σ_f values for undoped and 16-nitrogen-atom-doped UNCD. In addition, although SCC-DFTB predicts E accurately for undoped UNCD, it also predicts that SCD and undoped UNCD have the same Young's modulus. It has been shown using PBE that SCD has a larger E value than undoped UNCD (E=1.09 versus 1.05 TPa).[26]

Each of the three methods predicts a qualitatively different fracture path. PBE//MSINDO predicts the fracture of the bottom GB in Fig. 1(a), leaving four nitrogen atoms at its top and bottom. PBE and SCC-DFTB both predict the fracture of the top GB, leaving two nitrogen atoms at its top and six at its bottom. However, PBE and SCC-DFTB predict bond-breaking between different pairs of atoms in some cases.

Nevertheless, PBE//MSINDO and SCC-DFTB both predict reasonable E and ϵ_f, usually within several percent of the PBE values. They agree less well with PBE in their σ_f predictions but the force near where bond breaking occurs is difficult to calculate accurately; even the PBE values are somewhat questionable. These findings are consistent with the results of a related study in which semiempirical quantum and DFT calculations of the fracture of carbon nanotubes with defects were compared.[37]

Experience suggests that SCC-DFTB and PBE//MSINDO roughly perform equally well for UNCD-cluster problems. One advantage of SCC-DFTB is that its implementation requires a single-stage calculation while PBE//MSINDO requires the execution of two different codes. Although run times of the two methods are strongly dependent on the number of geometry optimization cycles required for convergence, they are usually similar.

IV. REALISTIC GRAIN BOUNDARIES FOR NITROGEN-PLASMA UNCD

As mentioned in the introduction, UNCD produced with high levels of nitrogen in the plasma (>5%) has a morphology which is significantly different than that produced in the absence of nitrogen. The most significant differences are an increase in the average diameter of diamond grains (increased to ~16 nm) and an increase in the width of the GB's between them (increased to ~2 nm). As the mechanical properties of SCD have already been studied extensively,[22,25] we focus our attention on the mechanical properties of the GB's.

We have created a model of a plasma-nitrogen GB, which is based on the Σ 13 GB structure of Fig. 1(a). The intention was to create a ~1-nm-wide GB between two pieces of SCD, with an sp^2 fraction close to that observed experimentally. Starting from the Σ 13 structure, 11 atoms have been removed from the SCD section between the two atom-wide GB's. The top and bottom four planes of atoms were not disturbed. Atoms were removed at random but subject to the constraint that removal leads to sp^2 hybridization. After PBE geometry optimization, this new 1.0-nm-wide GB (shown in Fig. 3) was found to contain 44% sp^2 carbon (as compared to a 47% sp^2 experimental data-based estimate for the films). The remainder of the atoms are sp^3 hybridized. This hybridization estimate is based on the number of nearest neighbors within 2.0 Å of a given atom. The top and bottom three planes of atoms were not included in this estimate, as they are SCD like and meant to represent the edges of grains. The hybridization of the atoms in these planes is 100% sp^3.

This GB structure is not unique in that other structures with a similar sp^2 hybridization percentage could also be constructed by the selective removal of atoms. However, care was exercised to remove atoms as uniformly as possible, so as to produce no large voids and to prevent the formation of carbon atoms with *sp* hybridization. As the investigation described in Sec. III indicates, the mechanical properties of the GB will be at least somewhat effected by the details of the atomic structure.

No nitrogen atoms have been included in the model shown in Fig. 3 which contains 119 GB atoms. As the calculation in Sec. I indicates, experimental 20% plasma-nitrogen films are approximately 29% GB by volume. In our model, there are 78 atoms in 6/16 of the unit cell volume which gives a density of 208 atoms/(unit cell volume) in the SCD regions. There are 119 atoms in 10/16 of the unit cell volume which gives a density of 190.4 atoms/(unit cell volume) in the GB region. If there are 119 GB atoms in a given volume (making up 29% of the total volume), consideration of the differences in densities leads one to expect ~318 SCD atoms in the other 71% of this volume, resulting in a total of 437 atoms. At experimentally observed doping levels of between 1 and 2 nitrogen atoms per 1000 carbon atoms one would, therefore, expect between 0 and 1 nitrogen atom to be in a cluster containing 119 GB atoms.

The structure shown in Fig. 3 has been strained to failure using PBE//MSINDO, SCC-DFTB, and PBE. The results are presented in Fig. 4 and Table III. The three methods provide a fairly consistent picture of how the mechanical properties of the Σ 13 structure change when additional defects are introduced. As Table III indicates, *E* is significantly smaller for the cluster in Fig. 3 than for UNCD produced with no plasma nitrogen. This is expected as the new structure contains a significant number of defects which are larger than those present in the Σ 13 structure. The fracture stress, although markedly reduced, is still large, with the PBE method predicting a value 61% of that for the original structure. The other two methods predict similar reductions in σ_f (values are reduced to 74% and 52% of the Σ 13 values for PBE//MSINDO and SCC-DFTB, respectively). Modest reductions in ϵ_f (of ~15%) are predicted by PBE//MSINDO and SCC-DFTB while PBE predicts no change.

TABLE II. Calculated mechanical properties of undoped and nitrogen-doped UNCD.

Cluster	*E* (TPa)	ϵ_f	σ_f (GPa)
UNCD (PBE//MSINDO)	0.95	0.16	116
UNCD (PBE)	1.05	0.13	100
UNCD (SCC-DFTB)	1.08	0.18	135
4 N atoms (PBE//MSINDO)	0.93±0.02[a]	0.17±0.02	107±7
8 N atoms (PBE//MSINDO)	0.91	0.15	90
16 N atoms (PBE//MSINDO)	0.94	0.11	84
16 N atom (PBE)	0.99	0.09	73
16 N atom (SCC-DFTB)	0.98	0.10	83
32 N atoms (PBE//MSINDO)	0.87	0.11	79

[a]Error bars reflect the size of the standard deviation in the values for the five clusters which contain four nitrogen atoms.

As in the case of the 16-nitrogen-atom-doped cluster, the three methods predict fracture paths which are significantly different from one another. In the PBE//MSINDO simulations, the cluster breaks close to the bottom of the defected region. About half of this region (atoms in planes 8–11) is heavily involved in fracture. The cluster breaks, leaving a string of five atoms extending from the bottom towards the

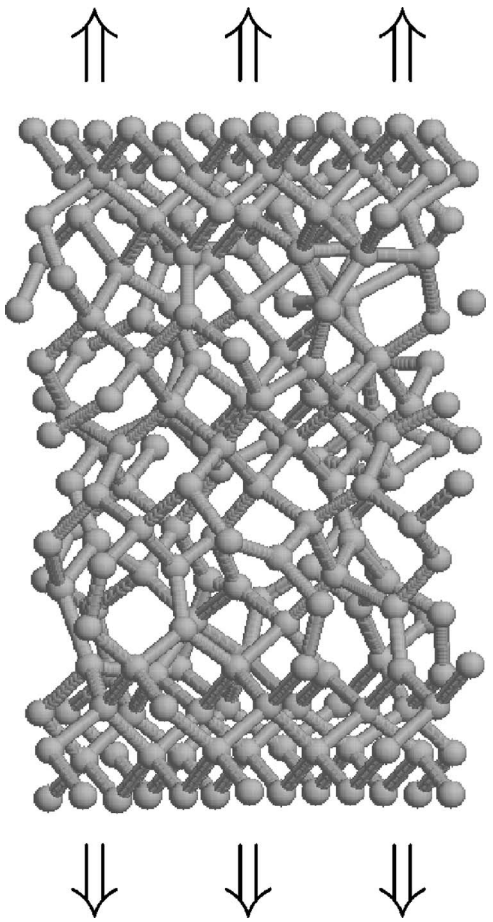

FIG. 3. The cluster used to model UNCD produced with nitrogen in the plasma. The arrows indicate the direction of applied strain.

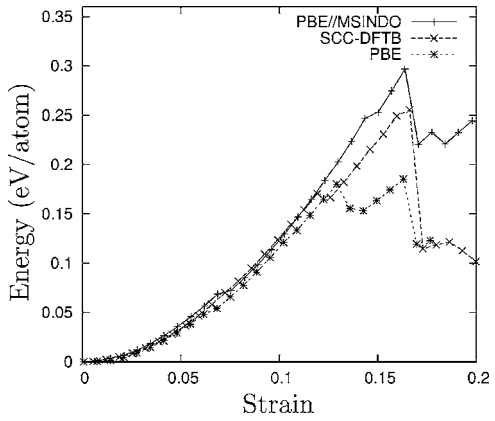

FIG. 4. The energy versus strain behavior of the cluster shown in Fig. 3, as calculated using PBE//MSINDO, SCC-DFTB, and PBE.

top of the structure. In the SCC-DFTB simulations, the cluster fractures closer to the middle of the defected region (involving predominantly atom planes 7 and 8), leaving two short strings of atoms extending from the lower to upper fragments of the structure. Finally, in the PBE simulations the cluster begins to fracture close to the top of the defected region (disrupting predominantly atoms in atom-planes 5 and 6). Once a crack opens in this region, it proceeds towards the center of the GB region, resulting in a 16-atom fragment of the right side of the GB remaining attached to the top section of SCD. However, for the most part, fracture occurs between the lowest SCD-like atom layer (layer 4) and the atoms in the defected region.

Comparisons indicate that the calculated E values are consistent with those observed experimentally. The experimental values are $E=0.95$ and 0.85 TPa for UNCD produced without and with high-level plasma nitrogen, respectively.[5,19] Our simulations predict a larger difference in E values ($E=1.05$ TPa versus 0.69 TPa for UNCD produced without and with plasma nitrogen, respectively, as predicted using the PBE method). This difference may be due to the fact that in experimental samples of UNCD, SCD regions much larger than the ones considered in the model shown in Fig. 3 (with associated larger E values) are placed under strain. This should result in a larger effective E value for experimental plasma-nitrogen UNCD than predicted by our model. This effect will be less pronounced for UNCD produced in the absence of plasma nitrogen because the Young's modulus of its atom-wide GB's is very close to that of SCD (Ref. 26) ($E=1.05$ TPa versus 1.09 TPa).

The tensile fracture stress of our modeled plasma-nitrogen UNCD ($\sigma_f=61$ GPa) is much larger than that observed experimentally[19] ($\sigma_f=2-3$ GPa). It has been suggested, based on results of atomistic simulations, that this discrepancy for a diamond GB is due to large defects and can be explained using the Griffith formula.[38] Previously, we have suggested that the large discrepancy between the Σ 13 model and the experimental fracture stress of UNCD produced in the absence of nitrogen can be plausibly explained by defects with length scales much larger than those considered in our computer models and indicated experimental evidence for such defects.[26] We will refer to these as "large-scale defects." The Griffith equation for a penny-shaped crack of radius c gives the fracture stress as[27]

$$\sigma_f = \left(\frac{\pi E \gamma}{2c(1-\nu^2)}\right)^{1/2}, \tag{2}$$

where γ is the fracture surface energy and ν is the Poisson ratio.

Griffith theory is quite effective in estimating σ_f for covalently bonded nanostructures since the principal mode of failure is bond breaking: our calculations have shown no evidence of dislocation emission at the crack tip. Thus the major source of error in the Griffith formula is the nonlinearity in the stress-strain curve. Although lattice trapping effects can also lead to errors in Griffith formula predictions, these are quite modest for long-range bonding forces such as those in carbon.

Intergranular failure (i.e., failure of GB's) dominates UNCD fracture.[19] Therefore, we computed the surface energy by separating the top section of SCD (layer 4) from the top GB layer (layer 5), as this is roughly the path along which failure occurs in our PBE simulations. The two sections are separated from each other by 0.9 nm, relative to their original positions (the size of the unit cell is increased accordingly), geometry optimized using PBE simulations, and then the energy of the resulting structure calculated.

This structure differs somewhat from that which results from the full-PBE-strain-to-failure, described earlier. In the structure resulting from strain-to-failure, additional rearrangements of atoms occur as strain is applied, before failure occurs. We use the energy associated with the structure just described, and not that of the structure resulting from the full-strain calculation, as the former is more in the spirit of Griffith brittle fracture.

The computed surface energy is 2.8 J/m^2, which differs only a little from the surface energy of UNCD produced without nitrogen in the plasma[26] ($\gamma=2.6$ J/m^2). There is some uncertainty associated with these surface energy estimates as their values depend on the structural details of the cluster models. The fact that the more highly defected plasma-nitrogen model is associated with a higher surface energy than the less defected model is somewhat surprising. However, surface energies depend not only on the energy required to break chemical bonds, but also on the energy released as new ones are formed.

We have not calculated the Poisson ratio but expect it to be close to that of SCD (Ref. 22) ($\nu=0.07$) as more than 70% of the volume of plasma-nitrogen UNCD is made up of SCD grains.

TABLE III. Computed mechanical properties of plasma-nitrogen UNCD.

Method	E (TPa)	ϵ_f	σ_f (GPa)
PBE//MSINDO	0.78	0.14	86
PBE	0.69	0.13	61
SCC-DFTB	0.69	0.16	70

Experimental values of the fracture stress are in the range of 2–3 GPa. Based on our calculations of surface energy and Young's modulus and the Griffith formula, Eq. (2), this indicates that the size range of the maximum defect in the experimental specimens is on the order of $c=300-800$ nm. We note that in the specimens of Espinosa *et al.*,[6] defects with radii as large as $c\sim 300$ nm were observed, which is consistent with our estimate.

V. SUMMARY

The fracture properties of UNCD produced with high levels of plasma nitrogen have been investigated. Two types of models have been examined. In the first, we considered atom-wide grain boundaries similar to those appropriate for undoped UNCD, and we studied the effect of random substitutions of nitrogen for carbon at the GB. This led to small reductions in Young's modulus (6%), failure strain (31%), and tensile fracture stress (27%) based on PBE calculations with 16 nitrogen atoms. The second model of UNCD has several of the attributes of analogous experimental films, with wider GB's and no nitrogen substitution which can be associated with plasma-nitrogen UNCD. PBE calculations with this yielded Young's modulus ($E=0.69$ TPa), failure strain ($\epsilon_f=0.13$), and tensile fracture stress ($\sigma_f=61$ GPa).

Calculations were also made with the semiempirical quantum mechanical methods, SCC-DFTB, and PBE//MSINDO. The three methods provide a fairly consistent picture of the fracture process. The SCC-DFTB and PBE//MSINDO methods predict E, ϵ_f, and σ_f values which are within 14%, 23%, and 35% of the PBE values, respectively. However, the three methods predict significantly different fracture paths.

The fracture stress of nitrogen-plasma UNCD predicted by our models is very large compared to that observed experimentally. Using the Griffith formula with our calculations of surface energy, we have shown that the experimental tensile fracture stresses indicate defects which have length scales on the order of hundreds of nm. The defect size predicted by Griffith agrees with the defect size observed experimentally.

ACKNOWLEDGMENTS

We gratefully acknowledge grant support from the National Science Foundation (Grant No. CMS 500304472) and NASA University Research, Engineering and Technology Institute on Bio Inspired Materials (BIMat) under Award No. NCC-1-02037.

*Electronic address: jpaci@chem.northwestern.edu
†Electronic address: schatz@chem.northwestern.edu

[1] D. M. Gruen, S. Liu, A. R. Krauss, J. Luo, and X. Pan, Appl. Phys. Lett. **64**, 1502 (1994).
[2] L. C. Qin, D. Zhou, A. R. Krauss, and D. M. Gruen, Nanostruct. Mater. **10**, 649 (1998).
[3] D. M. Gruen, Annu. Rev. Mater. Sci. **29**, 211 (1999).
[4] X. Xiao, J. Birrell, J. E. Gerbi, O. Auciello, and J. A. Carlisle, J. Appl. Phys. **96**, 2232 (2004).
[5] H. D. Espinosa, B. C. Prorok, B. Peng, K. H. Kim, N. Moldovan, O. Auciello, J. A. Carlisle, D. M. Gruen, and D. C. Mancini, Exp. Mech. **43**, 256 (2003).
[6] H. D. Espinosa, B. Peng, B. C. Prorok, N. Moldovan, O. Auciello, J. A. Carlisle, D. M. Gruen, and D. C. Mancini, J. Appl. Phys. **94**, 6076 (2003).
[7] C. Zuiker, A. R. Krauss, D. M. Gruen, X. Pan, J. C. Li, R. Csencsits, A. Erdemir, C. Bindal, and G. Fenske, Thin Solid Films **270**, 154 (1995).
[8] A. Erdemir, G. R. Fenske, A. R. Krauss, D. M. Gruen, T. McCauley, and R. T. Csencsits, Surf. Coat. Technol. **120–121**, 565 (1999).
[9] B. Fausett, M. C. Granger, M. L. Hupert, J. Wang, G. M. Swain, and D. M. Gruen, Electroanalysis **12**, 7 (2000).
[10] S. Bhattacharyya, O. Auciello, J. Birrell, J. A. Carlisle, L. A. Curtiss, A. N. Goyette, D. M. Gruen, A. R. Krauss, J. Schlueter, A. Sumant, and P. Zapol, Appl. Phys. Lett. **79**, 1441 (2001).
[11] T. D. Corrigan, D. M. Gruen, A. R. Krauss, P. Zapol, and R. P. H. Chang, Diamond Relat. Mater. **11**, 43 (2002).
[12] J. Birrell, J. A. Carlisle, O. Auciello, D. M. Gruen, and J. M. Gibson, Appl. Phys. Lett. **81**, 2235 (2002).
[13] J. Birrell, J. E. Gerbi, O. Auciello, J. M. Gibson, D. M. Gruen, and J. A. Carlisle, J. Appl. Phys. **93**, 5606 (2003).
[14] J. E. Gerbi, O. Auciello, J. Birrell, D. M. Gruen, B. W. Alphenaar, and J. A. Carlisle, Appl. Phys. Lett. **83**, 2001 (2003).
[15] A. R. Krauss, O. Auciello, D. M. Gruen, A. Jayatissa, A. Sumant, J. Tucek, D. C. Mancini, N. Moldovan, A. Erdemir, D. Ersoy, M. N. Gardos, H. G. Busmann, E. M. Meyer, and M. Q. Ding, Diamond Relat. Mater. **10**, 1952 (2001).
[16] O. Auciello, J. Birrell, J. A. Carlisle, J. E. Gerbi, X. Xiao, B. Peng, and H. D. Espinosa, J. Phys.: Condens. Matter **16**, R539 (2004).
[17] G. Palumbo, S. J. Thorpe, and K. T. Aust, Scr. Metall. Mater. **24**, 1347 (1990).
[18] P. Zapol, M. Sternberg, L. A. Curtiss, T. Frauenheim, and D. M. Gruen, Phys. Rev. B **65**, 045403 (2001).
[19] H. D. Espinosa (private communication).
[20] H. J. McSkimin and P. Andreatch, Jr., J. Appl. Phys. **43**, 2944 (1972).
[21] M. H. Grimsditch and A. K. Ramdas, Phys. Rev. B **11**, 3139 (1975).
[22] J. E. Field and C. S. J. Pickles, Diamond Relat. Mater. **5**, 625 (1996).
[23] Q. Chen, D. M. Gruen, A. R. Krauss, T. D. Corrigan, M. Witek, and G. M. Swain, J. Electrochem. Soc. **148**, E44 (2001).
[24] J. Robertson and C. A. Davis, Diamond Relat. Mater. **4**, 441 (1995).
[25] R. H. Telling, C. J. Pickard, M. C. Payne, and J. E. Field, Phys. Rev. Lett. **84**, 5160 (2000).
[26] J. T. Paci, T. Belytschko, and G. C. Schatz, Chem. Phys. Lett. **414**, 351 (2005).

[27] T. L. Anderson, *Fracture Mechanics, Fundamentals and Applications* (CRC Press, Boca Raton, 1991).
[28] J. R. Reimers, Z.-L. Cai, A Bilić, and N. S. Hush, Ann. N.Y. Acad. Sci. **1006**, 235 (2003).
[29] D. Sánchez-Portal, P. Ordejón, E. Artacho, and J. M. Soler, Int. J. Quantum Chem. **65**, 453 (1997).
[30] J. M. Soler, E. Artacho, J. D. Gale, A. García, J. Junquera, P. Ordejón, and D. Sánchez-Portal, J. Phys.: Condens. Matter **14**, 2745 (2002).
[31] D. Porezag, Th. Frauenheim, Th. Köhler, G. Seifert, and R. Kaschner, Phys. Rev. B **51**, 12947 (1995).
[32] Th. Frauenheim, G. Seifert, M. Elstner, Th. Niehaus, C. Köhler, M. Amkreutz, M. Sternberg, Z. Hajnal, A. Di Carlo, and S. Suhai, J. Phys.: Condens. Matter **14**, 3015 (2002).
[33] B. Ahlswede and K. Jug, J. Comput. Chem. **20**, 563, 572 (1999).
[34] M. Sternberg, D. A. Horner, P. C. Redfern, P. Zapol, and L. A. Curtiss, J. Comput. Theor. Nanosci. **2**, 207 (2005).
[35] P. Keblinski, D. Wolf, S. R. Phillpot, and H. Gleiter, J. Mater. Res. **13**, 2077 (1998).
[36] J. T. Paci, L. Sun, T. Belytschko, and G. C. Schatz, Chem. Phys. Lett. **403**, 16 (2005).
[37] S. L. Mielke, D. Troya, S. Zhang, J.-L. Li, S. Xiao, R. Car, R. S. Ruoff, G. C. Schatz, and T. Belytschko, Chem. Phys. Lett. **390**, 413 (2004).
[38] O. A. Shenderova, D. W. Brenner, A. Omeltchenko, X. Su, and L. H. Yang, Phys. Rev. B **61**, 3877 (2000).